Trial fabrication of traveling-wave ultrasonic motor with alumina-based ring-shaped vibrator

リング型アルミナ製振動子を用いた進行波超音波モータの試作

Jiang Wu†, Yosuke Mizuno, and Kentaro Nakamura (Laboratory for Future Interdisciplinary Research of Science and Technology, Tokyo Institute of Technology)
ウー・ジャン†，水野洋輔，中村健太郎 (東京工業大学　未来産業技術研究所)

1. Introduction

Ultrasonic motors (USMs) have the advtanages of simple structures, high torques at low rotation speeds, and good response characteristics compared to electromagnetic motors [1]. Recently, actuators capable of working in acid/alkaline environments have become demanded as key compoents of robots used in the chemical industry [2]. However, current USMs are inapplicable because their vibrators are made of metals lacking chemical resisitance. In previous studies, we employed a functional polymer with low mechanical loss, i.e. ploy phenylene sulfide (PPS) [3], to substitute the metal parts of vibrators [4]. Relatively high rotation speeds and high power densities were obtained on polymer/PZT motors, but output torques were limited owing to the low Young's moduli of polymer materials [4]. In addition to polymers, rigid ceramics, e.g. alumina, zirconia, and silicon carbide, are potentially applicable to non-metal USMs because of not only acid/alkaline resistance but also their higher elastic moduli, which may lead to higher output torques and powers for motors [5]. Besides, since engineering ceramics generally have low densities, rigid-ceramic/PZT motors may provide high power densities. Thus, it would be meaningful to employ engineering ceramics as the vibrating bodies of motors.

In this study, we fabricate several ring-shaped vibrators with alumina and experimentally investigate their basic characteristics. Subsequently, we use these vibrators to form traveling wave USMs, and evaluate their performance.

2. Configuration

Fig. 1(a) schematically shows the developed motor. As depicted in **Fig. 1(b)**, the vibrator consists of an alumina vibrating body and an annular piezoelectric ceramic disk. The alumina vibrating body (A9951, NTK Ceratec) comprises a back disk 0.5 mm in thickness, and a cylindrical part 30 and 20 mm in outer and inner diameters, respectively. Slots with 1 mm depth and 0.5 mm width are created at a 10° interval on the cylindrical part. A central hole is introduced on the back disk to fix the vibrator. The material constants of the tested alumina are listed in **Table I**. A polar coordinate system (z-, θ-, and r-axes) is established on the upper surface. As shown in **Fig. 1(c)**, the piezoelectric ceramic disk (C213, Fuji Ceramics) has an outer diameter of 30 mm, an inner diameter of 20 mm, and a thickness of 0.5 mm. One side of the sliver electrode is evenly divided into 12 parts, which have the identical polarization directions. The undivided side is bonded to the back surface of the alumina vibrating body with epoxy resin. The ring-shaped aluminum rotor shown in **Fig. 1(d)** has two parts with different diameters. A bearing is inserted into the part with a 33 mm outer diameter, while the bottom surface of the part with a 30 mm outer diameter contacts the outer edge of the vibrator. A spring is used to apply a preload to the rotor to efficiently generate frictional force to drive the rotor.

Table I Material constants of alumina

Young's modulus	390 GPa
Density	3.9×10^3 kg/m^3
Poisson's ratio	0.24

3. Experimental results

First, we explored the optimal electrical parameters for driving the motors. **Fig. 2** plots the no-load rotation speed of the motor with the vibrator with a 3-mm-thick un-slotted part (t3 vibrator) as a function of the frequency. The applied voltage and preload between four channels were respectively 10 V and 3.3 N. Observably, the rotation speed reached approximately 16 rad/s, the maximal value, at 71.22 kHz. **Fig. 3** demonstrates how the no-load rotation speed changes as the phase is varied. When the phases were -90° and 100°, the motor provides its maximum rotation speeds along the clockwise and counterclockwise directions, respectively. The dead regions can be observed in the phase ranges between -180° and -160° and between 0 and 10°.

Subsequently, we evaluated the performance of the t3 motor when the voltgae, frequency, and phase were 10 V, 71.22 kHz, and 100°, respectively. As

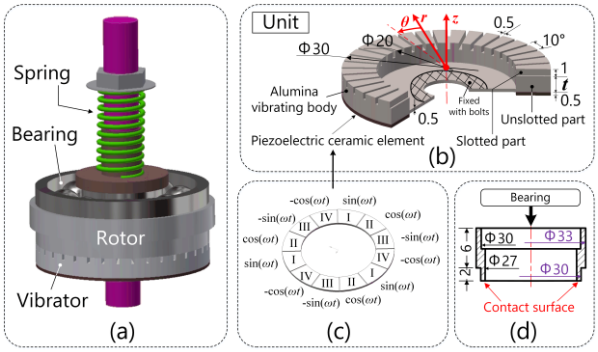

Fig. 1 (a) Configuration of motor, (b) piezoelectric ceramic element and its (c) electrode, and (d) rotor.

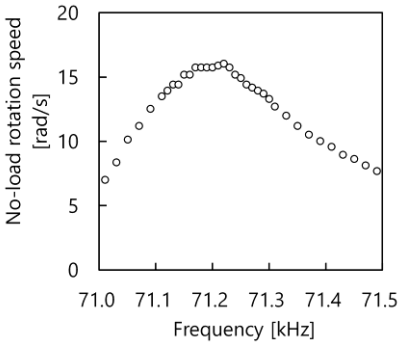

Fig. 2 No-load rotation speed versus frequency.

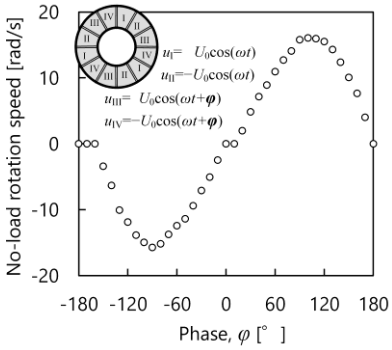

Fig. 3 No-load rotation speed versus phase.

shown in **Fig. 4(a)**, the rotation speed linearly decreased as the torque became higher. The maximum torque reached 12.8 mNm at the preload of 3.3 N. **Figs. 4(b)** and **(c)** demonstrated that the motor exhibited its maximum power and efficiency at moderate torques. At 3.3 N, the maximum power reached 58 mW and the maximum efficiency was approximately 6%. However, when the applied voltage exceeded 30 V, the vibrator fractured probably because the stress on the boundary between the vibrating body and the piezoelectric ceramic element was larger than the bond strength of the adhesive.

4. Conclusion

In this study, we tested several traveling-wave ring-shaped USMs with alumina vibrating bodies. The alumina/PZT motors successfully rotated as conventional metal/PZT ones. In particular, they could be driven at relatively low voltage compared to metal/PZT ones possibly owing to the high Young's modulus of alumina. In further studies, we will optimize the vibrator structures to obtain better performance. In addition, to achieve practical application of our motor to acid/alkaline environment, its accessory components, e.g. bearing and feeding line, will be carefully selected or specially designed.

Acknowledgment

This work was supported by JSPS KAKENHI 17J05057.

References

1. S. Ueha, Y. Tomikawa, M. Kurosawa, and K. Nakamura: Ultrasonic Motors-Theory and Applications (Oxford Univ. Press 1993), p. 4-13.
2. L. Zheng, S. Liu, and S. Wang: Int J. Mech. Eng Rob. Res. **5** (2016) 295.
3. J. Wu, Y. Mizuno, M. Tabaru, and K. Nakamura: Ultrasonics **69** (2016) 74.
4. J. Wu, Y. Mizuno, M. Tabaru, and K. Nakamura: Jpn. J. Appl. Phys. **55** (2016) 018001.
5. J. Wu, Y. Mizuno, and K. Nakamura: Smart Mater. Struct. **26** (2017) 115022.

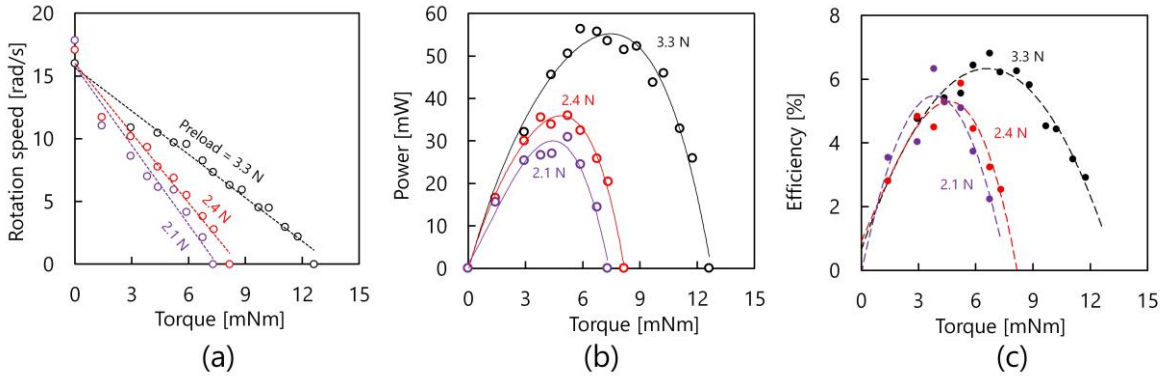

Fig. 4 Load characteristics: (a) Rotation speed, (b) output power, and (c) efficiency as a function of torque.